Elliptic flow in heavy ion collisions at varying energies: Partonic versus hadronic dynamics

Vincenzo Greco,[1,2] Michael Mitrovski,[3] and Giorgio Torrieri[4]

[1]*Department of Physics and Astronomy, Via S. Sofia 64, I-95125 Catania, Italy*

[2]*INFN Laboratori Nazionali del Sud, Via S. Sofia 62, I-95125 Catania, Italy*

[3]*Brookhaven National Laboratory, Upton New York 11973, USA*

[4]*FIAS, Johann Wolfgang Goethe Universität, Frankfurt, Germany*

We examine whether the breakdown in elliptic flow quark number scaling observed at the Relativistic Heavy Ion Collider (RHIC) energy scan is related to the turning off of deconfinement by testing the hypothesis that hydrodynamics and parton coalescence always apply, but are obscured, at lower energies, by variations in the widths of quark and antiquark rapidity distribution. We find that this effect is enough to spoil quark number scaling in elliptic flow. A lack of scaling in data, therefore, does not signal the absence of partonic degrees of freedom and hadronization by coalescence. In a coalescing partonic fluid, however, elliptic flow of antibaryons should be greater than that of baryons, since antibaryons contain a greater admixture of partons from the highly flowing midrapidity region. Intriguingly, purely hadronic dynamics has a similar dependence of baryon-antibaryons elliptic flow as purely partonic dynamics, again because antibaryons tend to come from regions where the deviation of the system from hydrodynamic behavior is at its smallest. The opposite trend observed in experiment is therefore an indication that we might be misunderstanding the origin of elliptic flow. We finish by discussing possible explanations of this and suggest experimental measurements capable of clarifying the situation.

I. INTRODUCTION

The discovery, at the Relativistic Heavy Ion Collider (RHIC), of a "perfect fluid" hadronizing via "quark coalescence" [1–7] has aroused a lot of experimental and theoretical attention. The main experimental evidence to support perfect fluidity is the observation that elliptic flow v_2, defined as the 2nd Fourier coefficient in the particle spectrum with respect to the reaction plane ϕ_{rp},

$$\frac{dN}{dy\,dp_T\,d\phi} = \frac{dN}{dy\,dp_T}\{1 + 2v_n\cos[n(\phi - \phi_{rp})]\}, \quad (1)$$

approaches the value expected from hydrodynamics [6]. The further scaling of mesonic and baryonic v_2 is suggestive of what is seen by the most naive quark coalescence:

$$\left(\frac{dN}{d^3p}\right)_{\text{hadron}} = \int d^3p_i \left[\prod_i \left(\frac{dN}{d^3p}\right)_{\text{quark}}\right]$$
$$\times W(x_i|x_{\text{hadron}}; p_i|p_{\text{hadron}}) \quad (2)$$

Provided the Wigner functions [8,9] $W(\ldots)$ are δ functions in position and momentum, $v_2^{\text{baryon}}(p/3)/3 = v_2^{\text{meson}}(p/2)/2$ [10], a relation that holds surprisingly well at the top RHIC energy of 200 GeV per nucleon [1–6], even if signs of finite width Wigner functions have been identified [7,11]. The most common interpretation of this is that the degrees of freedom carrying elliptic flow are partonic [7–13]. Coalescence of partonic degrees of freedom is also hinted by the high p_T baryon distribution [8,9] and can account for two-particle correlations structures such as the near-side "ridge" [12] and the far-side "cone" [14]. It has been found to significantly affect, also, the nuclear modification factor and the elliptic flow of heavy quarks [15,16].

It is, however, far from clear how the flow data and its "partonic ideal fluid" interpretation is related to the onset of deconfinement. In the confined phase, the coupling constant between mesons goes as λ/N_c^2 [17], while the density of degrees of freedom, impacting both viscosity η and entropy density s, goes as N_c^0. Hence, $\eta/s \sim N_c^2$. In the deconfined phase, the density of degrees of freedom goes as N_c^2; hence, $\eta/s \sim N_c^0$ independently of the coupling constant. η/s should, respectively, go to a constant for strongly interacting theories [18] or go as $\sim(\lambda^2 \ln\lambda)^{-1}$ in the perturbative regime [19], both $\sim N_c^0$. Hence, Simple number of colors scaling [17] shows that at deconfinement, η/s should jump by an order of magnitude. If elliptic flow is indeed hydrodynamically generated, a corresponding jump should be observed when the initial temperature is about the critical temperature for deconfinement [20,21]. No such jumps in the elliptic flow observable are apparent in experimental data, whether varied in center of mass energy, centrality, or rapidity [2,21,22].

Seeing how the v_2 observable "turns off" is indeed one of the objectives of making *lower* energy measurements with the latest detectors [23–26]. Recently, the RHIC experimental energy scan started observing a systematic breakdown of coalescence in $\sqrt{s}$ (not seen, so far, in rapidity [27]), which has been interpreted as signifying the "turning off" of partonic degrees of freedom [28,29]. However, as pointed out in Ref. [30], such a conclusion is premature: even if quark coalescence persists, high baryochemical potential and small rapidity intervals in the collision region might be enough to make it not apparent when v_2 of mesons and baryons is considered.

In this work we explore the consequences of the rapidity dependence of both dN/dy and $v_2(y)$ on the quark number scaling and on the baryon and antibaryons splitting of the elliptic flow, pointing out that recent observations of the RHIC

experiments at low energy are not explicable neither by a pure hydrodynamical+coalescence model nor by a pure hadronic model.

II. MODEL

Our model is simplified to capture the main issues we want to deal with. We assume *all* v_2 is produced in a close-to-ideal hydrodynamic stage at *all* energies.

The main consequence of an ideal hydrodynamics stage for our purposes is that, locally in rapidity and comoving time, flow u_μ is species independent. For configuration space coordinates $\vec{x}$, while *abundances* of flavors can vary,

$$u_\mu^q(\vec{x}) = u_\mu^{\bar{q}}(\vec{x}) = u_\mu^s(\vec{x}) = u_\mu^{\bar{s}}(\vec{x}). \quad (3)$$

This is simply a consequence of the fact that in ideal fluids any conserved current $J^\mu \propto u^\mu$, and deviations from this relation, are invariably dissipative [31]. This is *independent* of the initial condition for hydrodynamic evolution, allowing us to draw qualitative conclusions from an admittedly simplified schematic model.

Hence, before hadronization, provided flavor content is homogeneous in the transverse plane, for quarks emitted at rapidity y and transverse momentum p_T we have, up to mass corrections,

$$v_2^{q,s}(p_T, y) = v_2^{\bar{q},\bar{s}}(p_T, y), \quad \langle p_T \rangle^{q,s}(y) = \langle p_T \rangle^{\bar{q},\bar{s}}(y). \quad (4)$$

The other important ingredient to define the partonic stage is the y and p_T dependence of quark and antiquark distribution function. We assume a Gaussian antiquark distribution (Fig. 1),

$$\left(\frac{dN}{d^2 p_T \, dy}\right)_{\bar{q}} = N_{\bar{q}}^0 \exp\left[-\frac{y^2}{\sigma_y^2}\right] f(p_T, \phi), \quad (5)$$

where σ_y^2 is approximately $\sim \ln s$, growing from $\simeq \ln(s/2m_{\text{proton}})$ to $\simeq \ln(s/m_{\text{proton}})$ between the Landau and Bjorken limits [32,33].

For the quark distribution, we assume a flat distribution for a rapidity region $|y| < 1$, meaning the probability of finding
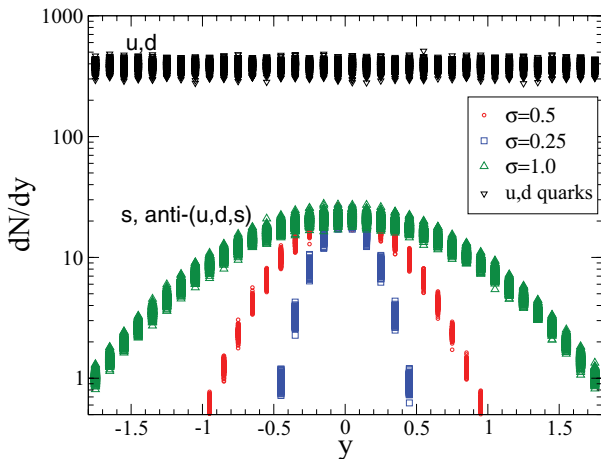

FIG. 1. (Color online) dN/dy of quarks and antiquarks. For antiquarks we plot the three widths employed in our studies: $\sigma_y = 0.25, 0.5, 1$.

a valence quark is approximately invariant with rapidity. This appears quite reasonable at least if the beam energy is $\sqrt{s} > 5$ GeV,

$$\left(\frac{dN}{d^2 p_T \, dy}\right)_q = N_q^0 f(p_T, \phi). \quad (6)$$

The normalization can be fixed by the $\bar{p}/p$ ratio,

$$\left(dN_{\bar{q}}^0/dy\right)/\left(dN_q^0/dy\right) \sim [(dN_{\bar{p}}/dy)/(dN_p/dy)]^{1/3}, \quad (7)$$

experimentally decreasing with $\sqrt{s}$, as more entropy is carried by pre-existing valence quarks rather than created $\bar{q}q$ pairs. Strange quarks and antiquarks distribution is the same as antiquarks, since they are produced from zero in the hot medium.

While these are undoubtedly simplified assumptions, more complicated scenarios [34] would, provided they model the experimentally observed limiting fragmentation of v_2 and dN/dy [21] and Eq. (3), give qualitatively similar results to those we present. This is because in any such system the bulk of antiquarks and strange quarks would come from a central plateau, whose width $\Delta y \leqslant 1$ grows very slowly with $\sqrt{s}$ [2,21]. The central plateau is also the region closest to ideal hydrodynamics, at all energies.

In accord with the hydrodynamic hypothesis for the quark phase, the momentum distribution is independent of the quark flavor ($q, \bar{q}, s, \bar{s}$ have the same $\langle p_T \rangle$ and v_2). Hence, a similar $f(p_T, \phi)$ describes both q and $\bar{q}$,

$$f(p_T, \phi) = e^{-\frac{m_T}{T}}[1 + 2v_2^p(p_T, y)\cos(2\phi)], \quad (8)$$

and $T = 170$ MeV. To fit experimental data [21,22], the quark (antiquark and strange quark) v_2 distribution for partons is also Gaussian:

$$v_2^p(p_T, y) = v_2(y = 0, p_T)e^{-\frac{y^2}{\sigma_y^2}}; \quad (9)$$

$v_2^p(y = 0, p_T)$ is an empirical function compatible with experimental data. Its integral is fixed by the experimental constraint [21] $v_2(y = 0)/\epsilon \sim (1/S)(dN/dy)$, where S is the overlap area of the collision $S \simeq (1 - \epsilon)\pi R^2$. $v_2(y > 0)$ is assumed, as seems to be the case in experimental data [1,2,27], to have the same σ_y as the "hot" medium (antiquark and strange quark distributions).

Note that even if $v_2(y, p_T)$ is the same for all partons *locally*, this is not true for $v_2(p_T)$ integrated over a finite y region. For example, in Fig. 2 we show $v_2(p_T)|_{|y| \leqslant 0.5}$ for quarks (up triangles) and antiquarks and strange quarks (down triangles) for two different widths.

This difference is due to the different dN/dy distributions for quarks and antiquarks together with the rapidity dependence of v_2. Antiquarks have the largest dN/dy from $y \sim 0$ region because at finite y dN/dy has a Gaussian-like tail

$$v_{2,\bar{q}}(p_T)|_{|y| \leqslant y^*} = \frac{\int_{-y^*}^{y^*} dy \, e^{-\frac{y^2}{\sigma_y^2}} v_2(p_T, y)}{\int_{-y^*}^{+y^*} dy \, e^{-\frac{y^2}{\sigma_y^2}}}. \quad (10)$$

Since v_2 is maximum at $y \sim 0$, this generally leads to $v_{2,q}(p_T) < v_{2,\bar{q}}(p_T)$. Since the Wigner function is also approximately a Gaussian, a similar mechanism acts also in the
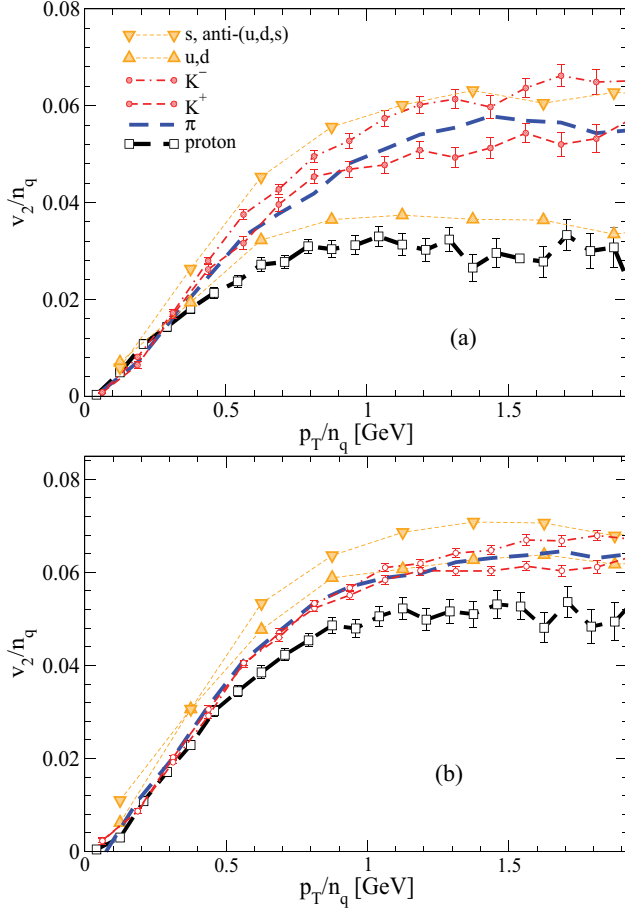
FIG. 2. (Color online) v_2/n_q vs. p_T/n_q of quarks, mesons baryons, and antibaryons in the $|y| \leqslant 0.5$ rapidity window and for two different σ values: Top panel (a) assumes $\sigma_y = 0.25$ and bottom panel (b) has $\sigma_y = 0.5$.

coalescence process leading to a smaller flow for mesons with both an $\bar{q}$ and an s quark, such as K^-, with respect to those having a $q\bar{q}$ or $q\bar{s}$.

To study the v_2 of hadrons in the p_T range $[0-5]$ GeV we assume coalescence-type hadronization that for the case of mesons is given by

$$N_M = C_M \int \prod_{i=a,b} (p \cdot d\sigma)_i \, d^4 p_i \, \delta(p_i^2 - m_i^2) f_i(r_i, p_i)$$
$$\times \, W(r \,|\, r_{\text{hadron}}; q \,|\, q_{\text{hadron}}). \quad (11)$$

The relative phase space coordinates $r = r_b - r_a$ and $q = p_b - p_a$ are the four-vector relative space-time distance and energy momentum. $d\sigma$ is a volume element of a spacelike hypersurface. The hypersurface of coalescing partons is fixed through the condition of equal longitudinal proper time $\tau = \sqrt{t^2 - z^2}$ [9,15]. In the coalescence integral in Eq. (11), we consider the full phase space overlap of the coalescing particles, with the advantage of avoiding some of the more restrictive approximations employed by other coalescence models. In particular, the extended 3D Wigner function avoids any collinear approximations in momentum.

The hadron Wigner function for light quarks used is a simple product of spheres in position and momentum space

$$W(r \,|\, r_{\text{hadron}}; q \,|\, q_{\text{hadron}})$$
$$= \frac{9\pi}{2} \Theta \big[\Delta_r^2 - (r - r_{\text{hadron}})^2 \big]$$
$$\times \, \Theta \big[\Delta_p^2 - (q - q_{\text{hadron}})^2 + (m_a - m_b)^2 \big]. \quad (12)$$

The radii Δ_r and Δ_p in the Wigner formalism obey the relation $\Delta_p = \Delta_r^{-1}$, motivated by the uncertainty principle. Similar expression can be derived for three-quarks coalescence. The parameter Δ_p is taken to be different for baryons and mesons and is of the order of the Fermi momentum, $\Delta_p^M = 0.23$ GeV and $\Delta_p^B = 0.35$ GeV. This has been shown to account for both the π, K, p, $\bar{p}$, Λ spectra at RHIC energy and quark number scaling elliptic flow, including its small baryon and meson breaking [11,35,36]. The condition for the four-vector relative momentum can be written as

$$(p_{T,a} - p_{T,b})^2 - 2 m_{T,a} \, m_{T,b} \cosh(y_a - y_b)$$
$$- m_{T,a}^2 - m_{T,b}^2 < \Delta_p^2; \quad (13)$$

in the nonrelativistic limit $|\vec{p}| \ll m_i$, this reduces to the condition $(\vec{p}_a - \vec{p}_b)^2 \leqslant \Delta_p$, i.e., that the relative momentum, and hence also the difference in rapidity, of the coalescing quarks is limited to the width of the hadron wave function.

In the ultrarelativistic limit $|\vec{p}| \gg m_i$, Eq. (13) reduces to

$$2 \, p_{T,a} \, p_{T,b} [\cos(\phi_a - \phi_b) + \cosh(y_a - y_b)] < \Delta_p^2, \quad (14)$$

which implies that at large p_T, due to the Lorentz boost from the fireball frame to the coalescing quark frame, particles with relatively large $\Delta p = |p_{T,a} - p_{T,b}|$ can coalesce. This effect [11] follows from relativistic kinematics and leads in our case to an increasing difference between particle and antiparticle $v_2(p_T)$ as a function of p_T.

While in previous work the elliptic flow of coalescence was studied considering flat distribution in rapidity, we show that in the presence of a finite Wigner function in Eq. (2) and a y-dependent anti-quark density the naive quark number scaling breaks down and a difference in baryon-antibaryon v_2 appears *even if ideal partonic hydrodynamics and coalescence occur at all energies*. While such a scenario is usually assumed not to apply for lower energies (this is very different from "demonstratively falsified"), it is worthwhile to estimate the magnitude of these effects.

III. RESULTS

The meson and baryon v_2's are summarized in Fig. 2. As can be seen, the $v_n(p_T/n_q)/n_q$ naive scaling is considerably broken when q-$\bar{q}$ asymmetry is broken and the width of distribution is sufficiently narrow. When $\sigma_y^2 = 0.25$, the proton v_2/n_q is below the meson one by nearly 50% while the antiproton one is above it. K^+ and K^- are similarly very different, while the difference between Λ and $\bar{\Lambda}$ is smaller (see Fig. 3), because the difference comes only from one over three quarks instead of one over two. All of these can be readily explained by the greater admixture of high-flow antiquarks and strange quarks in antibaryons and strange hadrons. In the
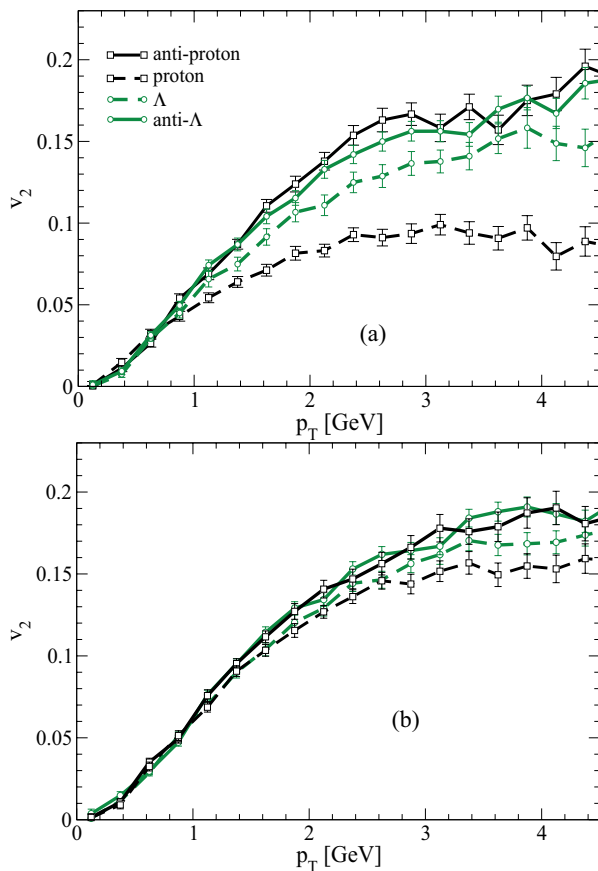
FIG. 3. (Color online) v_2 of baryons and antibaryons calculated in the rapidity region $|y| \leqslant 0.5$. The antiquark and strange quark distribution is a Gaussian with width in rapidity of, respectively, $\sigma_y = 0.25$ [top panel (a)] and $\sigma_y = 0.5$ [bottom panel (b)].

$K^-(s\bar{u})$, for instance, *both* quarks tend to come from smaller $|y|$ where the flow is larger, while in K^+ only one does. Hence, $K^+(u\bar{s})$ has a higher $v_2(p_T)$. Up to an asymmetry of $\sigma_y = 0.5$, the breaking of the scaling is still sizable but start to emerge when the transverse momentum per constituent quark is $\geqslant 1$ GeV. With $\sigma_y \geqslant 1$, the usual scaling are essentially restored. We notice that in a realistic description, thermal smearing should also be included, destroying the "locality" in momentum rapidity of the parton distribution and mixing quarks from flowing central region with the more baryon-rich fragmentation region. This effect with $\Delta y \simeq 0.5$ produces a similar effect to the one we have investigated for coalescence with finite width wave function; therefore, the lowering of baryon v_2 would persist even if $\Delta_{\text{Wigner}} \rightarrow 0$ as long as $\bar{p}/p$ breaks boost invariance.

Our other main result, shown in Fig. 3, is that v_2 is higher for antibaryons than for baryons. The difference is noticeable at all p_T if the width in rapidity of the antiquark and strange quark distribution is 0.25 but becomes noticeable at higher $p_T \sim 2$ GeV only if the width increases to $\simeq 0.5$. A further increase of the width makes the limiting p_T of the difference even higher.

This result is stable against changes in the details of parton distributions as long as Eq. (3) and the decreasing $\bar{q}/q$ as

a function of rapidity are valid assumptions, since baryons admit an admixture of quarks from the high rapidity peripheral regions, where v_2 is smaller, while antibaryons are dominated by central rapidity region at larger v_2. Any coalescence incorporating finite width wave function will result in a higher v_2 for antibaryons with respect to baryons. However, this directly contradicts experimental data [28], suggesting either that coalescence breaks down at lower energies or that quarks and antiquarks do not have the same flow $v_2(y, p_T)$.

IV. DISCUSSION

At this point one may ask if at lower energy what we have created is just a pure hadron gas. The systematics of $v_2(p_T)$, overlapping for all accessible momenta between $\sqrt{s}$ of 7.7 GeV and LHC energies [29], makes different regimes of v_2 origin immediately suspect. Nevertheless, to investigate this possibility we have calculated the v_2 of protons and antiprotons in purely hadronic molecular dynamics, implemented via the UrQMD model [37].

It should be noted that the version we used, v2.3 [38], suffers, as in earlier versions, from lack of detailed balance for multiparticle reactions: annihilation processes involving multiparticle final states, such as $p\bar{p} \rightarrow \pi\pi\pi\pi$, are possible. The corresponding creation processes, however, are absent. Quantitatively, this is a minor correction, since its equilibration time for $2 \leftrightarrow n$ processes $\tau_{n \leftrightarrow 2} \sim e^{n-2}\tau_{2 \leftrightarrow 2}$, and, as uRQMD shows, even $2 \leftrightarrow 2$ processes do not equilibrate in realistic heavy ion collision expansion profiles. However, in high chemical potential systems, antiprotons are also minor corrections, being suppressed by factors of $\sim \exp(-(m + \mu_B)/T)$, so the *relative* importance of multiparticle processes could become enhanced.

The uRQMD result is shown in Fig. 4, for the upper and lower physically relevant energies [28], it has a *similar* behavior to purely partonic dynamics + coalescence.

The reason this happens is, however, somewhat different: antiprotons are produced initially and get absorbed by annihilation in a proton-rich medium. Neglecting regeneration, it is not surprising that in a hadronic medium protons and antiprotons propagate differently: their thermally averaged
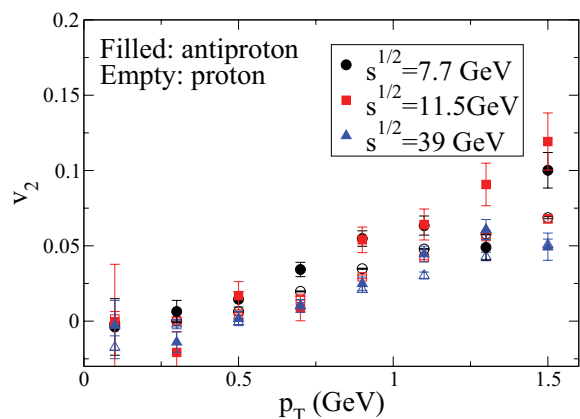

FIG. 4. (Color online) v_2 of p and $\bar{p}$ at 7.7, 11.5, and 39 GeV for 0–80% calculated within UrQMD.

interaction cross-sections are considerably different, since protons typically interact via resonance formation while antiprotons, in a high chemical potential medium, can interact *both* via resonance formation and collisional processes and annihilation, with the latter dominating if the Knudsen number is large and v_2 is created by absorption rather than flow. This, however, already makes it likely that antiprotons be *more* anisotropic, both due to flow and absorption, simply because they interact more with the medium.

Once again, naive extrapolation seems to disagree with experimental data [28], *neither* purely hadronic dynamics nor the coalescence hadronization of a partonic fluid. Dunlop and coworkers [30] proposed to explain this by assuming v_2 of particles transported from high rapidity is *higher* than the v_2 of particles created at midrapidity. It is, however, difficult to see how such an ansatz is compatible with the scaling of v_2 with rapidity [2,21], since "transported" degrees of freedom have to come, and spend more time in, *less* flowing regions. Our work confirms, in fact, that both partonic and hadronic dynamics, considering longitudinal diffusion *only*, have the opposite dependence on rapidity than that claimed in [30].

As shown in Ref. [39], *transverse* ideal hydrodynamics, incorporating instant chemical and thermal equilibrium for all hadronic species, might provide a way out, via chemical composition anisotropy in the transverse plane. If flow is created close to the ideal hydrodynamic limit, outer regions in transverse space have significantly more flow than inner-lying regions. The $\overline{p}/p \sim e^{-2\mu_B/T}$ ratio, however, decreases with transverse radius since most $\overline{p}$ are formed in the higher density inner regions: in the outer regions, μ_B is approximately the same but T goes down, depleting the $\overline{p}/p$ ratio.

As shown in Ref. [39], this effect can drive v_2 of protons above v_2 of antiprotons. However, coalescence in this case is also not ruled out, since by exactly the same reasoning, given a partonic system with q-$\overline{q}$ transverse anisotropy, one can drive the mean flow of quarks above the mean flow of antiquarks, effectively relaxing the assumption of Eq. (4), $v_{2q}(y) = v_{2\overline{q}}(y)$: *locally in transverse space* flow is, of course, still the same for all species, but the inhomogeneity leads to different transverse-averaged flows. Figure 5 shows what
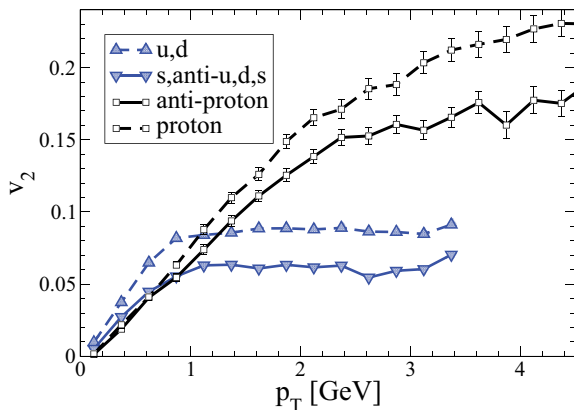

FIG. 5. (Color online) Plot of baryon vs. antibaryons v_2 with same parameters as described in the legend of Fig. 3 (upper panel) but with a modified width for quark; see text for details.

happens if the effective v_{2q} is just 20% of those of the antiquarks, a comparable effect to that used in Ref. [39] (the exact magnitude of the q-$\overline{q}$ transverse anisotropy should be approximately insensitive to whether uRQMD or "partonic" initial conditions are used). Partonic chemical nonequilibrium at freeze-out might accentuate this imbalance [40], since at $\mu_B \gg T$ light quarks equilibrate radiatively while light antiquarks equilibrate collisionally.

We conclude, therefore, that $2+1$ *partonic* hydro + coalescence might also be consistent with lower energies RHIC data if the transverse radius dependence of elliptic flow is taken into account. Since, as discussed previously, strange quarks are chemically similar to light antiquarks in that they are created thermally, we expect, if this scenario is correct, that

$$v_2^p - v_2^{\overline{p}} > v_2^{\Lambda} - v_2^{\overline{\Lambda}} > v_2^{\Xi} - v_2^{\overline{\Xi}} > v_2^{\Omega} - v_2^{\overline{\Omega}}, \quad v_2^{\Omega} \simeq v_2^{\overline{\Omega}}.$$

Alternatively, differential quark-antiquark flow can be directly realized in a system with either partonic or hadronic degrees of freedom *and* strong vector mean fields, since the repulsive channel at finite net quark number will generally be greater for q, s than $\overline{q}$, $\overline{s}$ (NB, both light and strange quarks). Vector mean fields, unlike scalar ones, can produce a difference between quarks and antiquarks because they admit both attractive and repulsive channels and are sensitive to a conserved charge density such as the net baryon or quark density.

In a medium with positive chemical potential, vector mean fields should cause relatively more attraction between antiparticles and the higher baryonic density regions and, therefore, a smaller $v_2(p_T)$ for antiparticles with respect to the particles. As shown in Ref. [41], within Boltzmann transport theory an attractive mean field causes a significant reduction of the $v_2(p_T)$. This can ultimately be related, in a hydrodynamical picture, to the fact that an attractive mean field decreases the effective pressure of the system at equilibrium. While elliptic flow is thought to be driven by pressure gradients, it remains to be clarified up to what level the transport and hydrodynamic picture are equivalent.

At hadronic level, the vector mean fields are ultimately how the AMPT calculation in Ref. [42] has been able to reproduce both the baryon and antibaryon v_2 data.

A model with *quark* mean fields has also been recently conjectured and studied within NJL [41] and PNJL models [43]. As Refs. [44–46] have shown, quark degrees of freedom coupled to mean fields can produce sizable elliptic flows [41,47], which, in a vector channel, can again vary considerably between quarks and antiquarks.

If, in the partonic system, the effect of mean fields is comparable to isotropic pressure, however, the very definition of thermalization and η/s needs to be revised, since defining a comoving frame within a strong mean field is impossible: particles and antiparticles will always move in different directions within a volume element, exactly the effect required to explain energy scan data. This also means that if v_2 is driven by mean fields, one would expect the difference between baryon and antibaryon v_2 to be constant with strangeness, since QCD dynamics is flavor-blind:

$$v_2^p - v_2^{\overline{p}} \simeq v_2^{\Lambda} - v_2^{\overline{\Lambda}} \simeq v_2^{\Xi} - v_2^{\overline{\Xi}} \simeq v_2^{\Omega} - v_2^{\overline{\Omega}}.$$

This latter scenario, however, leads to some unsettling questions for the interpretation of v_2 at *higher* energies: since at $\overline{p}/p \simeq 1$ such effects become invisible (C-symmetry of the medium is restored), there is no indication that they actually turn off at RHIC/LHC, and the smoothness of the decrease of the $v_2^p - v_2^{\overline{p}}$ with $\sqrt{s}$ [28] suggests they do not. As mean fields are "large" deviations from the hydrodynamic limit, discovering that they have a contribution to *creating* (rather than suppressing) v_n could significantly modify viscosity estimates such as those at higher energies [6].

To constrain the models further using existing data, let us consider that the *total* (π, K, p) $v_2(p_T)$ in the same energy scan can be experimentally shown [29] to be approximately independent of the initial density (which depends, approximately, as $\frac{1}{S}\frac{dN}{dy} \sim N_{\mathrm{part}} \ln \sqrt{s}$ [2], assuming Bjorken expansion [33] with a constant starting time); the integrated v_2 varies because $\langle p_T \rangle$ increases systematically with $\frac{1}{S}\frac{dN}{dy}$, but $v_2(p_T)$ overlaps within error bar [29].

The analysis in Fig. 4 also fails to reproduce such a scaling specifically for protons, in line with the interpretation of absorption as the dominant origin of v_2; in this case, the v_2 scaling with p_T should be governed by the collision integral formula of Ref. [48], where transverse density enters both into $\langle p_T \rangle$ and $v_2(p_T)$ via

$$v_2(p_T) \sim \langle \sigma v_{ij}(p_T) \rangle \left(\frac{\epsilon}{S} \frac{dN}{dy} \right). \qquad (15)$$

Here, $\langle \sigma v_{ij}(p_T) \rangle$ is the normalized cross-section times negative velocity for *that particular transverse momentum*. Neglecting averaging over rapidity, and assuming $d\sigma_{ij} \sim \alpha_{ij} dp_{TJ}^2 / Q^4$, where Q is the momentum transfer and p_{TJ} is the momentum of the second scatterer, we get

$$v_2(p_T) \sim \epsilon \frac{dN}{dy} f \left(\frac{p_T}{\langle p_T \rangle} \right) \frac{G(p_T)}{S}$$

$$G(p_T) = \alpha_{ij} \int_0^{2\pi} d\phi \int_0^\infty f \left(\frac{p_{TJ}}{\langle p_T \rangle} \right)$$

$$\times \frac{p_{TJ} dp_{TJ}}{\left[p_T^2 + p_{TJ}^2 - 2 p_T p_{TJ} \cos(\phi) \right]^2}, \qquad (16)$$

where we used the universal scaling of the transverse momentum distribution with $p_T/\langle p_T \rangle$ noted in Ref. [49], and $f(\ldots)$ is a distribution function, which can be well approximated by a Tsallis spectrum [50].

The $G(p_T)$ term generally breaks the scaling, increasing $v_2(p_T)$ by virtue of an increase in $\langle p_T \rangle$ with $\sqrt{s}$, N_{part} and decreasing $v_2(p_T)$ at the high $p_T \gg \langle p_T \rangle$ tail. In case of high baryochemical potential limit at low $\sqrt{s}$, the averaging of $\langle p_T \rangle$ over $p, \pi, K, \ldots$ and α_{ij} over $p - p, p - \pi, \pi - \pi, \ldots$ further breaks the scaling. This systematic shift is also visible in Fig. 11 of Ref. [29] or in Ref. [51] within the uRQMD and AMPT models, as $v_2(p_T)$ increases systematically with $\sqrt{s}$. The same reasoning explains the systematic rise specific to $p, \overline{p}$ observed in Fig. 4.

However, as explicitly discussed in Refs. [52,53], but also clear in Refs. [6,54], an ideal fluid stage creating v_2 via azimuthally inhomogeneus pressure gradients will *not* ameliorate this problem, since a Cooper-Frye freeze-out [55]

will result in a v_2, which to leading order depends on the 2nd Fourier components of the freeze-out hypersurface $\epsilon_2^{\Sigma_T}$ and transverse flow $\epsilon_2^{v_T}$ via

$$v_2(p_T) \sim \left\langle \tanh \left[\frac{\gamma \epsilon_2^{v_T} p_T}{T} \right] \left(1 - p_T \epsilon_2^{\Sigma_T} \right) \right\rangle \qquad (17)$$

and the averaging $\langle \ldots \rangle$ is done over events at a given $\sqrt{s}$ and centrality class.

Since both $\epsilon_2^{\Sigma_T}$ and $\epsilon_2^{v_T}$ depend on the lifetime of the system (albeit approximately saturate after a finite time [56]), $v_2(p_T)$ should also systematically rise with $\sqrt{s}$. The systematic deviation should increase with p_T, since both $\epsilon_2^{\Sigma_T, v_T}$ come with factors p_T. Such a behavior is indeed evident in Ref. [6] and is qualitatively the same as the transport simulation [51].

In recent years it has been pointed out that an agreement with data for several observables even at the highest RHIC energy can be better explained if one introduces a core-corona model [57]. The fact that AMPT, which incorporates both hadronic and partonic components in the relevant energy density regimes, has the same qualitative dependence as Ref. [6] (as seen in Fig. 11 in Ref. [29]) indicates that a core-corona model might find it challenging to reproduce $v_2(p_T)$ for all energies, since the greater preponderance of the corona at lower $\sqrt{s}$ should also change the p_T dependence of v_2 (v_2 in the corona is either zero or hadronic). However, since a core-corona model with an ideal core ($\eta/s = 0$) does a good job of reproducing integrated v_2/ϵ at several top energies and centralities [57], and $\eta/s = 0$ is expected to scale the best [20], perhaps the scaling of v_2 will, to a certain extent, survive when binned in p_T. This can be expected also on the base of dynamical transport calculations that include the strong η/s increase at hadronic energy densities [58]. Regarding the baryon/antibaryon pattern of $v_2(p_T)$, we have shown in the present paper that both a partonic and a hadronic picture show the same baryon/antibaryon pattern. Therefore, we can say that also employing a core-corona picture, the issue raised might persist unless strong transverse gradients within the core, a la Ref. [39], are maintained. It is, therefore, difficult to see whether either a hybrid analysis of a uRQMD-only analysis can accommodate the difference between p and $\overline{p}$ as well as the near-overlap of $v_2(p_T)$ seen in Ref. [29]. This near-overlap has not, however, as yet been established for separate particle species, so perhaps baryonic v_2 is quantitatively different from π-dominated total v_2. In this case, hydrodynamic evolution with a long hadronic afterburner [39] might be the simplest explanation of elliptic flow systematics.

In conclusion, we used quark coalescence and a simple parametrization of a quark fireball with hydrodynamic flow to investigate the dependence of coalescence-type scaling at various energies. We concluded that it is wrong to expect coalescence to give the naive quark number scaling of v_2 at all energies and system sizes *even if partonic hydrodynamics and coalescence actually occur*. We have also found that both coalescence and hadronic dynamics predict the opposite difference of baryon and antibaryon v_2 with respect to experimental data. The scaling of baryonic v_2, therefore, points to the existence of separate quark and antiquark flow at lower energies. A theoretical explanation of this will be

essential to link flow dynamics in heavy ion collisions to the deconfinement phase transition and this is presently missing.

[1] I. Arsene *et al.* (BRAHMS Collaboration), Nucl. Phys. A **757**, 1 (2005).

[2] B. B. Back *et al.*, Nucl. Phys. A **757**, 28 (2005).

[3] J. Adams *et al.* (STAR Collaboration), Nucl. Phys. A **757**, 102 (2005).

[4] K. Adcox *et al.* (PHENIX Collaboration), Nucl. Phys. A **757**, 184 (2005).

[5] M. Gyulassy and L. McLerran, Nucl. Phys. A **750**, 30 (2005).

[6] H. Song, S. A. Bass, U. Heinz, T. Hirano, and C. Shen, Phys. Rev. Lett. **106**, 192301 (2011).

[7] R. J. Fries, V. Greco, and P. Sorensen, Annu. Rev. Nucl. Part. Sci. **58**, 177 (2008).

[8] R. J. Fries, B. Muller, C. Nonaka, and S. A. Bass, Phys. Rev. C **68**, 044902 (2003).

[9] V. Greco, C. M. Ko, and P. Levai, Phys. Rev. C **68**, 034904 (2003).

[10] D. Molnar and S. A. Voloshin, Phys. Rev. Lett. **91**, 092301 (2003).

[11] V. Greco, Eur. Phys. J. ST **155**, 45 (2008).

[12] R. C. Hwa and C. B. Yang, Phys. Rev. C **66**, 025205 (2002).

[13] A. Adare *et al.* (PHENIX Collaboration), Phys. Rev. Lett. **98**, 162301 (2007).

[14] V. Greco, G. Torrieri, J. Noronha, and M. Gyulassy, Nucl. Phys. A **830**, 785 (2009).

[15] V. Greco, C. M. Ko, and R. Rapp, Phys. Lett. B **595**, 202 (2004).

[16] H. van Hees, M. Mannarelli, V. Greco, and R. Rapp, Phys. Rev. Lett. **100**, 192301 (2008).

[17] G. 't Hooft, Nucl. Phys. B **72**, 461 (1974).

[18] P. Danielewicz and M. Gyulassy, Phys. Rev. D **31**, 53 (1985).

[19] P. B. Arnold, G. D. Moore, and L. G. Yaffe, JHEP **11** (2000) 001.

[20] H. Song and U. W. Heinz, Phys. Rev. C **78**, 024902 (2008).

[21] G. Torrieri, Phys. Rev. C **82**, 054906 (2010).

[22] G. Torrieri, Phys. Rev. C **76**, 024903 (2007).

[23] M. Posiadala (NA61 Collaboration), arXiv:0901.3332.

[24] A. N. Sissakian and A. S. Sorin (NICA Collaboration), J. Phys. G **36**, 064069 (2009).

[25] M. M. Aggarwal *et al.* (STAR Collaboration), arXiv:1007.2613 [nucl-ex].

[26] P. Staszel (CBM Collaboration), Acta Phys. Pol. B **41**, 341 (2010).

[27] F. Videbaek (BRAHMS Collaboration), Nucl. Phys. A **830**, 43C (2009).

[28] S. Shi (STAR Collaboration), Acta Physica Polonica B Proceedings Supplement **5**, 311 (2012).

[29] L. Adamczyk *et al.* (STAR Collaboration), arXiv:1206.5528 [nucl-ex].

[30] J. C. Dunlop, M. A. Lisa, and P. Sorensen, Phys. Rev. C **84**, 044914 (2011).

[31] B. Betz, G. S. Denicol, T. Koide, E. Molnar, H. Niemi, and D. H. Rischke, EPJ Web Conf. **13**, 07005 (2011); G. Denicol, D. Rischke *et al.* (in preparation).

[32] C. Y. Wong, arXiv:0809.0517 [nucl-th].

[33] J. D. Bjorken, Phys. Rev. D **27**, 140 (1983).

[34] J. Letessier and J. Rafelski, J. Phys. G **28**, 183 (2002).

[35] V. Greco and C. M. Ko, Phys. Rev. C **70**, 024901 (2004).

[36] V. Greco, C. M. Ko, and I. Vitev, Phys. Rev. C **71**, 041901 (2005).

[37] M. Bleicher *et al.*, J. Phys. G **25**, 1859 (1999); S. A. Bass *et al.*, Prog. Part. Nucl. Phys. **41**, 255 (1998).

[38] H. Petersen, M. Bleicher, S. A. Bass, and H. Stocker, arXiv:0805.0567 [hep-ph].

[39] J. Steinheimer-Froschauer, V. Koch, M. Bleicher, Phys. Rev. C (in press); J. Steinheimer-Froschauer (private communication).

[40] K. Dusling, G. D. Moore, and D. Teaney, Phys. Rev. C **81**, 034907 (2010).

[41] S. Plumari, V. Baran, M. Di Toro, G. Ferini and V. Greco, Phys. Lett. B **689**, 18 (2010).

[42] J. Xu, L.-W. Chen, C. M. Ko, and Z.-W. Lin, Phys. Rev. C **85**, 041901(R) (2012).

[43] N. M. Bratovic, T. Hatsuda, and W. Weise, arXiv:1204.3788 [hep-ph].

[44] V. Koch, Nucl. Phys. A **830**, 479C (2009).

[45] T. S. Biro, M. Gyulassy, and Z. Schram, Phys. Lett. B **708**, 276 (2012).

[46] E. L. Bratkovskaya, W. Cassing, V. P. Konchakovski, O. Linnyk, V. Ozvenchuk, and V. Voronyuk, J. Phys. Conf. Ser. **316**, 012027 (2011).

[47] V. Greco, C. M. Ko, S. Plumari, and T. Song (in preparation).

[48] H. Heiselberg and A.-M. Levy, Phys. Rev. C **59**, 2716 (1999).

[49] R. C. Hwa and C. B. Yang, Phys. Rev. C **67**, 064902 (2003).

[50] T. S. Biro and B. Muller, Phys. Lett. B **578**, 78 (2004).

[51] D. Solanki, P. Sorensen, S. Basu, R. Raniwala, and T. K. Nayak, arXiv:1210.0512 [nucl-ex].

[52] G. Torrieri, B. Betz, and M. Gyulassy, AIP Conf. Proc. (in press).

[53] G. Torrieri, B. Betz, and M. Gyulassy (in preparation).

[54] E. Schnedermann, J. Sollfrank, and U. W. Heinz, Phys. Rev. C **48**, 2462 (1993).

[55] F. Cooper and G. Frye, Phys. Rev. D **10**, 186 (1974).

[56] J. Y. Ollitrault, Phys. Rev. D **46**, 229 (1992).

[57] J. Aichelin and K. Werner, J. Phys. G **37**, 094006 (2010).

[58] G. Ferini, M. Colonna, M. Di Toro, and V. Greco, Phys. Lett. B **670**, 325 (2009).